International Journal of Biological Macromolecules 79 (2015) 903–912

Contents lists available at ScienceDirect

International Journal of Biological Macromolecules

journal homepage: www.elsevier.com/locate/ijbiomac

Structural and functional studies of Hsp70-escort protein – Hep1 – of *Leishmania braziliensis*

P.R. Dores-Silva[a], L.L. Beloti[a], K. Minari[a,b], S.M.O. Silva[a], L.R.S. Barbosa[c], J.C. Borges[a,*]

[a] Institute of Chemistry of São Carlos, University of São Paulo – USP, São Carlos, SP 13560-970, Brazil
[b] Post-Graduation Program in Evolutionary Genetics and Molecular Biology, Federal University of São Carlos – UFSCar, São Carlos, SP 13565-905, Brazil
[c] Institute of Physics, University of São Paulo – USP, São Paulo, SP 05508-090, Brazil

ARTICLE INFO

Article history:
Received 18 March 2015
Received in revised form 22 May 2015
Accepted 23 May 2015
Available online 10 June 2015

Keywords:
Heat shock proteins
mtHsp70
Biophysical studies
Leishmania braziliensis

ABSTRACT

Hep1 is a mitochondrial Hsp70 (mtHsp70) co-chaperone that presents a zinc finger domain essential for its function. This co-chaperone acts to maintain mtHsp70 in its soluble and functional state. In this work, we have demonstrated that *Leishmania braziliensis* mtHsp70 (LbmtHsp70) is also dependent on the assistance of Hep1. To understand the *L. braziliensis* Hep1 (LbHep1) structure–function relationship, we produced LbHep1 and two truncated mutants corresponding to the C-terminal zinc finger domain and the N-terminal region. We observed that LbHep1 is composed of an unfolded N-terminal region and a β-sheet-folded C-terminal domain, which holds the zinc-binding motif. Both LbHep1 and the zinc finger domain construction maintained LbmtHsp70 solubility in co-expression systems after cell lysis. In solution, LbHep1 behaved as a highly elongated monomer, probably due to the unfolded N-terminal region. Furthermore, we also observed that the zinc ion interacted with LbHep1 with high affinity and was critical for LbHep1 structure and stability because its removal from LbHep1 solutions altered the protein structure and stability. *In vitro*, LbHep1 protected, in sub-stoichiometric fashion, LbmtHsp70 from thermally induced aggregation but did not present intrinsic chaperone activity on model client proteins. Therefore, LbHep1 is a specific chaperone for LbmtHsp70.

© 2015 Elsevier B.V. All rights reserved.

1. Introduction

Leishmaniasis is a neglected tropical disease that is caused by a protozoan of the genus *Leishmania* spp. and is transmitted by the bite of sand fly mosquitoes. Annually, Leishmaniasis is diagnosed in 1.6 million people distributed throughout 98 countries and because it can cause destruction of mucous membranes and internal organs, it is lethal in untreated severe forms [1].

During its digenetic life cycle, the parasites must to adapt to the temperature of the environment (insect vector, approximately 25 °C) and the mammalian host (37 °C) [2]. This temperature change triggers a *de novo* protein synthesis in the parasite, leading to an increased expression of molecular chaperones like Hsp90 and Hsp70 [3–5], in a mechanism dependent on their mRNA stability [6]. These proteins play critical roles in protozoal differentiation and adaptation processes and, alter sandfly promastigote development to amastigotes in the mammalian host [2,7]. Molecular chaperones also directly influence parasite virulence and survival inside mammalian host macrophages and assist in protozoa defense against oxidative stress and drug resistance [5,8]. Accordingly, molecular chaperones are the first cellular defense in bacteria and eukaryotes, and they act to specifically to prevent aggregation and correct misfolded proteins, thus maintaining protein homeostasis [9].

Among all molecular chaperone families, Hsp70 is one of the largest and most versatile and are highly expressed in a state of cellular stress [10,11]. In eukaryotes, Hsp70 are present in several cellular compartments such as the cytosol, nucleus, endoplasmic reticulum, mitochondria and chloroplasts, and many of these Hsp70 are essential for cell viability [11].

Notably, mitochondria are critical for eukaryotic cell survival. Apart from energy production and biosynthesis of essential

Abbreviations: AUC, analytical ultracentrifugation; CD, circular dichroism; D_{max}, maximum dimension; MM, molecular mass; Rs, Stokes radius; R_0, Stokes radius for a smooth and spherical particle; Rg, radius of gyration; *s*, sedimentation coefficient; $s_{20,w}$, sedimentation coefficient at standard conditions; $s^0_{20,w}$, standard sedimentation coefficient at 0 mg/mL of protein; s_{sph}, sedimentation coefficient for a smooth and spherical particle; SAXS, small-angle X-ray scattering; f/f_0, frictional ratio; [Θ], residual molar ellipticity; <λ>, center of spectral mass.

* Corresponding author at: Institute of Chemistry of São Carlos, University of São Paulo – USP, P.O. Box 780, 13560-970 São Carlos, SP, Brazil. Tel.: +55 16 3373 8637; fax: +55 16 3373 9982.
E-mail address: borgesjc@iqsc.usp.br (J.C. Borges).

http://dx.doi.org/10.1016/j.ijbiomac.2015.05.042
0141-8130/© 2015 Elsevier B.V. All rights reserved.

metabolites, they are responsible for several cellular processes such as cell cycle signaling, stress response and apoptosis [12]. In this context, mitochondrial Hsp70 (mtHsp70) drives the import of proteins that were synthesized in the cytoplasm (pre-proteins) to the mitochondrial matrix, assists in their correct folding [13] and prevents aggregation like most Hsp70 do [14–16].

Although mtHsp70 prevents protein aggregation, it has the propensity to self-aggregate [17,18]. Therefore, for mtHsp70 to remain functional even *in vitro*, it requires mtHsp70-escort protein-1 (Hep1 is also known as Tim15/Zim17/DNLZ), which acts as an mtHsp70 co-chaperone [18,19]. This co-chaperone is approximately 17 kDa and presents a zinc-binding motif (ZBM), which is critical for its *in vivo* function [20,21]. It is present in mitochondria and chloroplasts of all eukaryotes; however, it has not yet been reported in bacteria. The deletion of yeast Hep1 (yHep1) causes a pleiotropic effect, including temperature growth deficiency [22,23], which could be explained by deficient SSC1 activity (yeast mtHsp70), suggesting that the primary function of Hep1 proteins is to maintain mtHsp70 structure and function [19]. The same protective effect was observed with human mtHsp70 (HspA9/mortalin) [17] and chloroplast Hsp70B of *Chlamydomonas reinhardtii* [24,25]. Interestingly, a Hep1 ortholog called Zinc ribbon (ZR) protein was found in *Arabidopisis thaliana*, indicating that Hep1-like proteins are present in mitochondria and plastids of plants, animals, fungi and protists but not bacteria [26].

mtHsp70 is dependent on Hep1 to develop its proper functions; thus Hep1 inactivation can damage both the mitochondria and the chaperone network that assist in the adaptation of the parasite to the mammalian host directly and/or indirectly. Therefore, Hep1 can be a target for mtHsp70 inactivation. Taking these into account, our study aimed to structurally and functionally characterize, the *L. braziliensis* Hep1 (LbHep1) using biochemical and biophysical techniques. LbHep1 functionality and its N- and C-terminal truncated regions were assessed by its ability to maintain mtHsp70 *L. braziliensis* (LbmtHsp70) solubility in co-expression systems. The results demonstrated that recombinant LbHep1 behaves as a highly elongated monomer in solution, and the presence of zinc ions is essential for LbHep1 structural stability. In addition, the C-terminal region, which contains the ZBM, is largely responsible for LbHep1 structural content and function on LbmtHsp70 solubility and aggregation prevention in the recombinant production.

2. Materials and methods

2.1. DNA amplification and cloning

Genomic DNA from *L. braziliensis* was used for amplifying LbmtHsp70 (Genbank acc. no. XP_001566868) and LbHep1 encoding DNA (Genbank acc. no. XM_001565523) by polymerase chain reaction using specific primers containing site restrictions for specific endonucleases (Table S1 – Supplementary material). The forward primers were designed to exclude the mitochondrial peptide signal, which were predicted by the MITOPROT program [27]. The coding DNA for mature LbmtHsp70 (residues 21-651) was cloned into pET28a expression vector, while DNA for mature LbHep1 (45-220) as well as its N- and C-terminal regions LbHep1N (45-131) and LbHep1C (132-220) were cloned into both pET23a (for co-expression assays with LbmtHsp70 – see below) and pET28a (for protein production and purification) expression vectors. DNA sequencing confirmed the identity of the DNA inserts cloned in the expression vectors (data not shown).

2.2. Primary structure sequence alignment of LbHep1

The primary structure of LbHep1, yHep1/Zim17 and hHep1 were obtained from the NCBI database (Genbank acc. no: XP_001565573.1; NP_014089.2; NP_001074318.1, respectively), and the alignment was performed using ClustalW software (http://www.ebi.ac.uk/Tools/msa/clustalw2/).

2.3. LbHep1 and truncation mutants expression and purification

LbHep1, LbHep1C and LbHep1N constructs were expressed in the *Escherichia coli* BL21 (DE3) strain. The cells were grown at 37 °C and 200 rpm in LB broth containing kanamycin (30 μg mL^{-1}). When the cells achieved an OD_{600nm} of 0.6–0.8, 0.2 mM IPTG was added to initiate protein expression and incubated at 30 °C and 200 rpm for 4 h (LbHep1 and LbHep1C) and 12 h (LbHep1N). The cells were harvested by centrifugation (3,000 × *g* for 10 min at 4 °C) and resuspended in buffer A (20 mM sodium phosphate, pH 7.5, containing 500 mM NaCl and 20 mM imidazole) plus 0.01 mg mL^{-1} lysozyme, DNase (5 U) and 2 mM β-mercaptoethanol and disrupted by sonication. The proteins were purified by Ni^{2+}-affinity chromatography and incubated with 1 U mg^{-1} thrombin for His-tag cleavage. Proteins were then applied onto a Superdex 200 16/60 column (GE Healthcare LifeSciences) in TKP buffer (25 mM Tris–HCl, pH 7.4, containing 50 mM NaCl, 5 mM sodium phosphate, 5 mM KCl and 2 mM 2-mercaptoethanol). Protein purity was assessed by 12% SDS-PAGE. LbHep1 and LbHep1C concentrations were determined spectrophotometrically using calculated extinction coefficients in native conditions. As the primary structure of LbHep1N does not contain any aromatic amino acids, its concentration was estimated by 15% SDS-PAGE scaled with different LbHep1C amounts. GelQuant software (http://biochemlabsolutions.com/GelQuantNET.html) was used to calculate the intensity of bands in the gel, providing pixel intensity values. Thus, it was possible to estimate the concentration of LbHep1N from a known concentration of LbHep1C on the same gel (Fig. S2).

2.4. LbHep1 and truncation mutant co-expression assays

The functional activity for LbHep1 and its N- and C-terminal regions was evaluated by its ability to maintain recombinant LbmtHsp70 when overexpressed by the pET28a expression vector in the soluble fraction. For this, expression and co-expression experiments as described by Dores-Silva et al. [18] were conducted using *E. coli* BL21 (DE3) cells that were transformed with pET28a::LbmtHsp70; pET28a::LbmtHsp70 + pET23a::LbHep1; pET28a::LbmtHsp70 + pET23a::LbHep1N and pET28a::LbmtHsp70 + pET23a::LbHep1C. All of the transformed cells were grown in LB medium containing kanamycin (30 μg mL^{-1}) and/or ampicillin (50 μg mL^{-1}).

2.5. Spectroscopy studies

The CD spectra of purified LbHep1, LbHep1N and LbHep1C proteins were obtained using a J-815 spectropolarimeter (Jasco Inc.) as previously described [17]. These proteins were analyzed in TKP buffer at concentrations ranging of 6–30 μM. The CD spectra for untreated and EDTA-treated LbHep1 (to eliminate the zinc ion) were collected at concentrations ranging from 8 to 12 μM. Zn^{2+} ion displacement was accomplished by exhaustive dialysis in TKP buffer containing 200 mM EDTA followed by further dialysis against TKP buffer only to remove EDTA. The CD spectra was converted to mean residue ellipticity and used for deconvolution using CDNN Deconvolution software.

Intrinsic fluorescence emission measurements were performed in an F-4500 fluorescence spectrophotometer (Hitachi) using a

10 mm × 2 mm path length cell with LbHep1 in TKP buffer at 20 °C. Fluorescence emission spectra were measured from 300 to 420 nm after excitation at 280 nm at LbHep1 concentrations ranging between 5 and 15 μM. The effect of Zn^{2+} release on LbHep1 structure was followed by intrinsic fluorescence emission at increasing EDTA concentration. The urea-induced unfolding experiments were performed with 15 μM LbHep1 prepared in TKP buffer in the absence and the presence of 10 mM EDTA at 20 °C after 60–120 min equilibrium time at room temperature. The intrinsic fluorescence emission data were analyzed by maximum fluorescence emission wavelength (λ_{max}) and spectral center of mass (<λ>), as previously described [18].

2.6. Hydrodynamic characterization

Analytical SEC experiments and Stokes radius (Rs) determination of the studied proteins were performed as previously described [18]. The standard protein mix was constituted by apoferritin (480 kDa – Rs 67 Å), γ-globulin (160 kDa – Rs 48 Å), BSA (67 kDa – Rs 36 Å), ovalbumin (45 kDa – Rs 29 Å) and carbonic anhydrase (29 kDa – Rs 24 Å) (Sigma–Aldrich). The frictional ratio (f/f_0) was estimated by the ratio of the experimental Rs to the radius of a sphere of the same molecular mass [28].

Sedimentation velocity analytical ultracentrifugation (SV-AUC) experiments were performed in a Beckman Optima XL-A analytical ultracentrifuge and analyzed as previously described [18]. In summary, LbHep1 was assessed at concentrations from 0.1 to 2 mg/mL in TKP buffer at 20 °C at 32,000 rpm (AN-60Ti rotor), and data were acquired at 230 nm. SedFit software (Version 12.1) [29] was used for a fitting routine, where the f/f_0 worked as a regularization parameter to obtain the c(S) curves and the standard sedimentation coefficients ($s_{20,w}$). The $s_{20,w}$ were determined as the maximum c(S) curve peaks at each protein concentration and was used to calculate the standard sedimentation coefficient by linear regression at 0 mg/mL protein concentration ($s^0_{20,w}$) [30]. The SedFit software estimated the $s_{20,w}$-values because the buffer viscosity ($\eta = 1.0145 \times 10^{-2}$ poise), density ($\rho = 1.0018\ g\ mL^{-1}$) and LbHep1 partial-specific volume ($V_{bar} = 0.721\ mL\ g^{-1}$) were supplied by the Sednterp software (sednterp.unh.edu/).

2.7. SAXS experiments

The small angle X-ray scattering (SAXS) experiments were conducted at the Brazilian Synchrotron Light Laboratory (LNLS, Campinas-SP, Brazil) as previously described [18]. The LbHep1 scattering curves were recorded at 2.5 mg mL^{-1} in TKP buffer. Samples and buffers were measured in frames of 60 and 300 s, and scattering curves of the buffers were subtracted from sample scattering curves taking into account their X-ray attenuation. Scattering curves are presented in absolute scale (cm^{-1}) using ultra-pure Milli-Q water as a standard [31]. For monodisperse systems, the forward scattering intensity $I(q \rightarrow 0)$ is related to the protein MM. The Guinier law was used to estimate both protein radius of gyration (Rg) and $I(0)$. The GNOM program [32] was used to calculate the pair distance distribution function, p(r), which can give information about protein size and shape.

2.8. Isothermal titration calorimetry assay

Isothermal titration calorimetry (ITC) was performed using an iTC200 microcalorimeter (GE Healthcare Life Sciences) to investigate the zinc ion interaction with LbHep1 as well as evaluate its thermodynamic parameters [33]. The zinc ion was removed from the LbHep1 protein by exhaustive dialysis as previously mentioned. The ITC assay was performed by titration of 18 2 μL aliquots of 200 μM zinc sulfate into 203.8 μL 14.5 μM LbHep1 zinc-free sample at 25 °C. Protein and ligand were prepared in 50 mM acetate buffer (pH 5.5) containing 25 mM NaCl. The enthalpy change for each injection was calculated by integrating the area under the peaks of the recorded time course of the power change. The heat associated with the injected dilution was determined from the baseline at the end of the titration and subtracted from the data. The data were analyzed using Microcal Origin software with the One Set of Sites curve-fitting model to calculate the apparent binding enthalpy change (ΔH_{app}), binding stoichiometry (n) and association constant (K_A). The apparent Gibbs energy (ΔG_{app}) and apparent binding entropy change (ΔS_{app}) were calculated using the following equation:

$$\Delta G_{app} = -RT \ln K_A = \Delta H_{app} - T\Delta S_{app} \quad (1)$$

2.9. Prevention of LbmtHsp70 aggregation by LbHep1

The LbmtHsp70 aggregation prevention by LbHep1 was monitored by light scattering at 320 nm in a 1 cm pathlength quartz cuvette for 66 min at 41 °C. For this assay, 3.0 μM LbmtHsp70 was used with sub-stoichiometric to stoichiometric concentrations of LbHep1 (0.03–6 μM), both proteins solved in TKP buffer. LbHep1 chaperone activity was assessed by analyzing its ability to prevent protein aggregation of some model proteins as previously described [34]. For that assay, samples containing 1 μM malate dehydrogenase (MDH) or luciferase (Luc) in the absence and the presence of LbHep1 at increasing concentrations (1–5 μM) in TKP buffer (pH 7.5) were incubated at 40 °C for 3 h, and protein aggregation was monitored by absorbance at 340 nm in a 96-well microplate. These assays were performed in triplicate.

3. Results and discussion

3.1. Description of the primary structure of LbHep1

Fig. 1A depicts the primary structure of LbHep1 aligned with its human and yeast orthologues. The mitochondrial peptide signal (MPS), which is highlighted in all sequences, is absent in the mature protein because it is cleaved after protein transport from the cytosol into the mitochondria. The ZBM in focus is highly conserved between species [35], in which the ZBM from LbHep1 has 44% and 52% of identity with yHep1 and hHep1, respectively. The similarity in ZBM is approximately 76%. The black arrows indicate the conserved tetracysteine motif that is predicted to coordinate zinc ion [21,22]. Some studies indicate that the tetracysteine motif is critical for the *in vivo* function of Hep1, probably because they coordinate the zinc ion, which maintains the protein structure [35]. Upstream to ZBM, LbHep1 displays an N-terminal region that is longer than that of yHep1 and hHep1, whereas the C-terminal extremity is similar in length despite low amino acid sequence conservation. The role of the long LbHep1 N-terminal is unknown. In our work, full-length mature LbHep1 (residues 45-220), truncation mutants LbHep1N (45-131) and LbHep1C (132-220), which covers the entire ZBM region, were produced for studying LbHep1 structure and function.

3.2. Expression and purification of LbHep1 and truncation mutants

Recombinant LbHep1 and truncation mutants (LbHep1C and LbHep1N) were produced and purified by two chromatography steps (described in section 3.3). Recombinant LbHep1 (Fig. 2A) was produced and purified at a satisfactory purity level >95%. The truncation mutants (see Fig. S1) were also purified satisfactorily; however, they did not give a reasonable yield (data not shown), which limited their study.

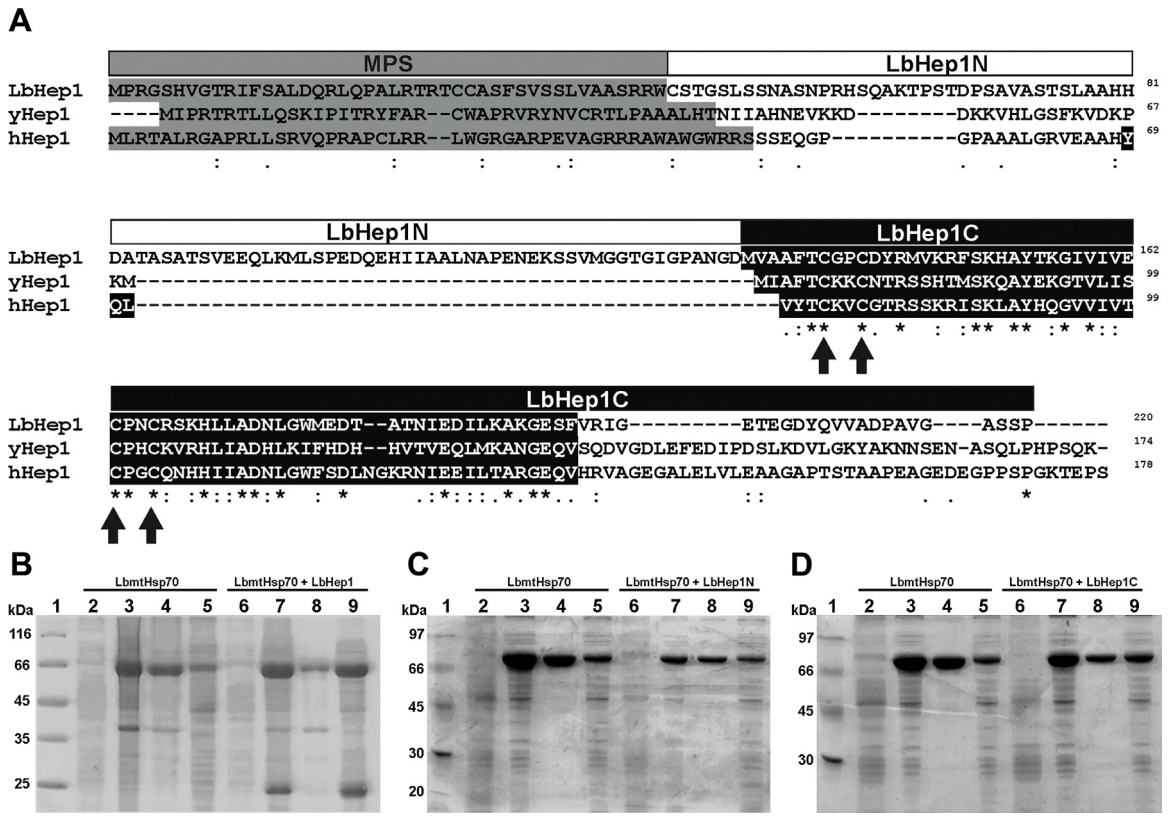

Fig. 1. LbHep1 primary structure and function on LbmtHsp70 solubilization. (A) LbHep1 alignment with yHep1 and hHep1, where the highlight indicates the mitochondrial peptide signal (MPS) (in gray) and the zinc-binding motif (ZBM) (in black). Arrows indicate the conserved tetracysteine motif. The degree of conservation among the amino acid residues is symbolized as follows: (*) all fully conserved residues; (:) one of the residues is fully conserved and [.] residues are weakly conserved. B–D) LbmtHsp70 (pET28::LbmtHsp70) expression and co-expression with LbHep1 (pET23::LbHep1), LbHep1N (pET23::LbHep1N) and LbHep1C (pET23::LbHep1C), respectively. (1) MM marker; (2) LbmtHsp70 non-induced cells; (3) LbmtHsp70-induced cells; (4) lysed cell pellet; (5) lysed cell supernatant; (6) not induced co-expression; (7) induced co-expression; (8) pellet of lysed cells with co-expression; (9) supernatant of lysed cells with co-expression. The results indicated the functionality of LbHep1 to solubilize LbmtHsp70 and suggest that LbHep1C present a major capacity to solubilize LbmtHsp70 compared with the LbHep1N region. Figure B was 15% SDS-PAGE and C and D were 12% SDS-PAGE.

3.3. LbHep1 and truncation mutants act solubilizing recombinant LbmtHsp70

yHep1 function was first analyzed *in vivo* following the aggregation of SSC1 and a defect in Fe/S protein biogenesis, thus allowing for the conclusion that yHep1 is not only required for mtHsp70 solubility but further assists the mtHsp70 interaction with client proteins in a J co-chaperone-dependent fashion [36]. Here, the ability of LbHep1 in solubilizing LbmtHsp70 was evaluated by co-expressing both proteins in the same *E. coli* BL21 (DE3) cell that was transformed with pET28a::LbmtHsp70 and pET23a::LbHep1 expression vectors, which were resistant to kanamycin and

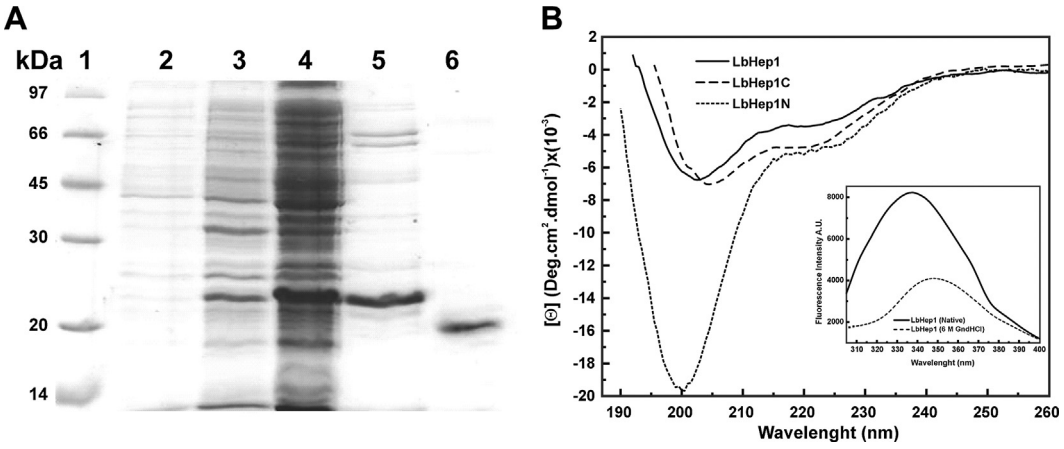

Fig. 2. LbHep1 purification as well as secondary and tertiary structure analysis. (A) 15% SDS-PAGE showing LbHep1 expression by pET28::LbHep1 vector and purification. Lane 1: MM standard. Lane 2: non-induced cells. Lane 3: pellet of induced cells after lysis. Lane 4: supernatant of induced cells after lysis. Lane 5: affinity chromatography fraction. Lane 6: size exclusion chromatography fraction after His-tag cleavage by thrombin. (B) CD and fluorescence spectra (inset) indicated the presence of secondary and tertiary structures, respectively. The deconvolution of the CD spectrum demonstrates that the protein presents a predominance of type β sheet structure. The CD data also depict that LbHep1-C construction has similar secondary structure to complete LbHep1, whereas the LbHep1-N has a CD spectrum profile of random structure. Inset: The fluorescence spectrum of LbHep1 demonstrates that its single tryptophan is partially exposed to solvent (see text for details).

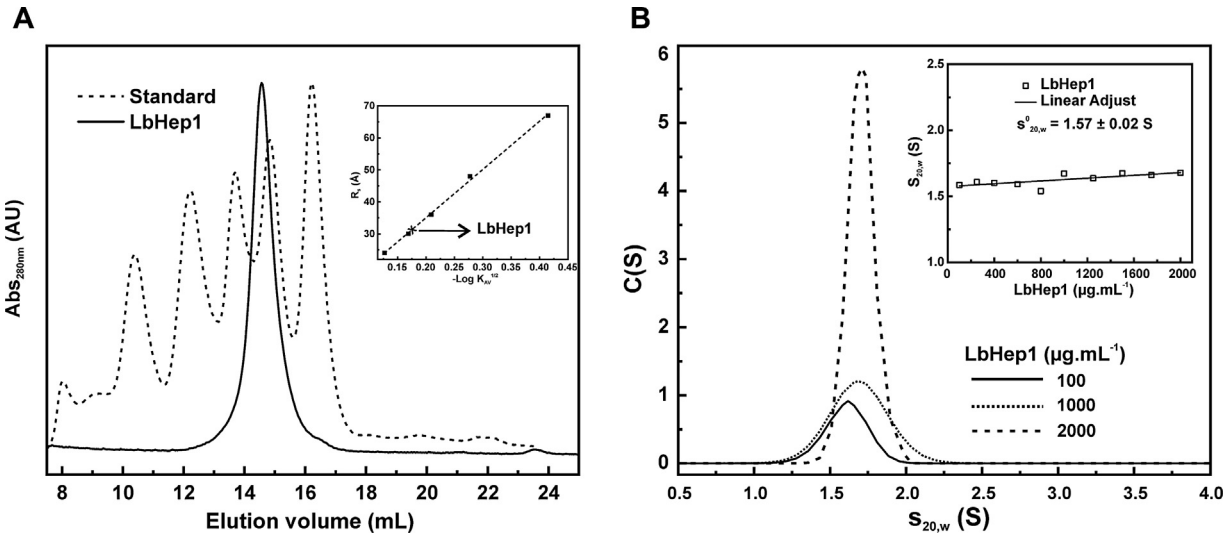

Fig. 3. LbHep1 is an elongated monomer in solution. (A) aSEC profile demonstrating that LbHep1 eluted with an equivalent elution volume between ovalbumin and BSA. The standard mix (dotted line), which was composed by apoferritin (480 kDa – Rs 67 Å), γ-globulin (160 kDa – Rs 48 Å), BSA (67 kDa – Rs 36 Å), ovalbumin (45 kDa – Rs 29 Å) and carbonic anhydrase (29 kDa – Rs 24 Å), allowed for the estimation of the Rs-value for LbHep1 of 31 ± 2 Å (*inset*). (B) SV-AUC experiments demonstrating that LbHep1 behaves as an apparent monodispersive solution with MM of 20 ± 1 kDa at concentrations in the range of 100–2,000 µg mL^{-1}. The $s_{20,w}$-values were plotted against the protein concentration allowing for estimating the value of the $s^0_{20,w}$ of 1.6 ± 0.1 S (*inset*). These experiments indicated that LbHep1 is an elongated monomer in solution.

ampicillin, respectively. Fig. 1B illustrates the co-expression results and the expression of LbmtHsp70 in the same conditions. When LbmtHsp70 was overexpressed alone, 70% of the protein remained in the insoluble fraction and only 30% remained in the soluble fraction, as analyzed by GelQuant software. However, when it was co-expressed with LbHep1, 80% of LbmtHsp70 was found in the soluble fraction and 20% was in the insoluble fraction. Thus, co-expression experiments demonstrated that LbHep1 presence is critical for solubilizing overexpressed LbmtHsp70. Similar effects were observed for hHep1 [18], yHep1 [37] and Hep2 of *C. reinhardtii* chloroplast [24]. Furthermore, a recent study reported that Hep1 proteins share sequence similarity with zinc ribbon-like (ZR) proteins of higher plants [26]. One of these ZR proteins (ZR3) complemented the function of mutant yHep1 and interacted with yeast mtHsp70 (SSC1) in co-precipitation assays. Despite the low sequence identity between Hep1 and ZR proteins, both have a ZBM [26]. Therefore, even phylogenetically distant, the biological function of Hep1 and ZR proteins are intimately related to organellar Hsp70 function. It can be speculated that Hep1 performs related functions across species is an endosymbiosis consequence.

As previously discussed, Hep1 has a ZBM in the C-terminal region [19]. To evaluate the role of the LbHep1 N- and C-terminal regions in LbmtHsp70 solubilization, we used LbHep1 truncation mutants in the co-expression experiments with LbmtHsp70 (Fig. 1C and 1D). Band intensity analysis on SDS-PAGE by the GelQuant Software indicates the LbHep1N was not effective in solubilizing LbmtHsp70 because 60% of its mass remained in the insoluble fraction and 40% was in the soluble fraction (Fig. 1C). In contrast, co-expression with LbHep1C resulted in partial solubilization of LbmtHsp70; 60% remained in the soluble fraction and 40% remained in the insoluble fraction (Fig. 1D). These results indicate that the LbHep1C region was effective in LbmtHsp70 solubilization, probably because it contains the ZBM (Fig. 1A). However, LbHep1C was less effective than full-length LbHep1, indicating that the LbHep1N region also contributes to this LbHep1 function. Similar findings have also been reported for hHep1 [20].

3.4. Recombinant LbHep1 has secondary and tertiary structures

The LbHep1, LbHep1C and LbHep1N secondary structures were evaluated by CD measurements (Fig. 2B). The LbHep1 CD spectrum indicated β-sheets as its main secondary structure content. Similar results were obtained for hHep1 [18] and for yHep1 [35]. In contrast, LbHep1N exhibited a single minimum at 200 nm, producing a large negative ellipticity that is typical of random coil proteins. The data for LbHep1C demonstrate a curve shape similar to LbHep1, indicating that the C-terminal region is responsible for the secondary structure that was observed for LbHep1. Similar results were also reported for hHep1 [20].

The presence of local tertiary structure was evaluated by intrinsic fluorescence emission because LbHep1 has one tryptophan residue in its primary structure in the same position as hHep1 (Fig. 1A). Fluorescence spectra demonstrated that LbHep1 has λ_{max} and <λ> centered at 336 ± 1 and 343.7 ± 0.2 nm, respectively, suggesting that its tryptophan is partially exposed to the solvent (Fig. 2B, *inset*). The chemical unfolding of LbHep1 induced by 6 M

Table 1
Summary of the hydrodynamic and structural data of LbHep1.

LbHep1 structural and hydrodynamic properties	Predicted for a sphere		Experimental determination		
	Monomer	Dimer	aSEC	AUC	SAXS
MM (kDa)	18.6	37	53 ± 4	20 ± 1	20 ± 1
$s^0_{20,w}$ (S)	2.25	2.65	–	1.57 ± 0.03	–
Rs (Å)	17	22	31 ± 2	–	–
f/f_0	1.0	1.0	1.8 ± 0.1[a]	1.7 ± 0.1	–
Rg (Å)	–	–	–	–	33 ± 1
D_{max} (Å)	–	–	–	–	130 ± 10

[a] By the ratio of the Rs determined from a SEC experiments by that predicted for a monomer.

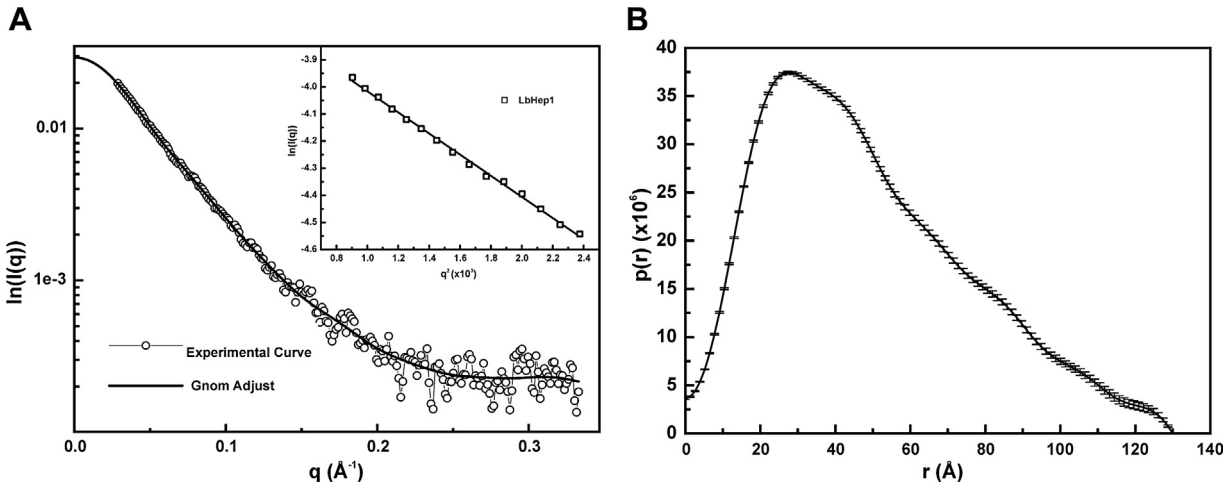

Fig. 4. Small-angle X-ray scattering of LbHep1. (A) Scattering curve of the LbHep1 at 2.5 mg mL^{-1} as well as the GNOM adjustment (black line). The Rg estimated experimentally was 33 ± 1 Å and MM calculated from the *I*(0)-value of 20 ± 1 kDa from the Guinier region (*inset*). (B) *p*(*r*) distribution curve of LbHep1 suggesting that the protein is highly elongated with D_{max} of about 130 ± 10 Å.

GndHCl led the λ_{max} and <λ> to 349 ± 1 and 351.7 ± 0.2 nm, respectively, attesting that LbHep1 has local tertiary structure.

3.5. LbHep1 behaves as a highly elongated monomer in solution

The hydrodynamic properties of LbHep1 were evaluated by means of analytical SEC experiments (Fig. 3). This experiment allowed for estimation of the apparent MM of 53 ± 4 kDa and Rs of 31 ± 2 Å (Fig. 3A and Table 1). These results indicated that LbHep1 could be an oligomer considering the predicted monomer MM of 18.6 kDa, or it could be an elongated molecule. To elucidate this issue, we used the SV-AUC technique in a large range of protein concentrations (0.2–2.0 mg mL^{-1}) (Fig. 3B). In contrast to that observed for hHep1 [18], LbHep1 solutions were monodisperse and had a MM of 20 ± 1 kDa for all of the protein concentrations analyzed. This result is in agreement with the predicted value for a monomer species (Table 1). Moreover, it presented a $s^0_{20,w}$ of 1.57 ± 0.03 S (Fig. 3B, *inset*) and a f/f_0 of 1.7, which was obtained from the SedFit analysis. Because LbHep1 is a monomer, the f/f_0 could also be obtained by the ratio between the experimental Rs and the predicted Rs and estimated from the protein MM as a monomer, and the value of f/f_0 of 1.8 ± 0.1 was registered for LbHep1 (Table 1). These results indicated that LbHep1 is a highly elongated molecule.

LbHep1 solution structure was also studied by means of SAXS experiments. Fig. 4A demonstrates the X-ray scattering curve and the GNOM fitting obtained for LbHep1. Using the Guinier approximation (Fig. 4A, *inset*), a MM of 20 ± 1 kDa and the Rg of 33 ± 1 Å for LbHep1 were found. Such MM values are in good agreement with an MM monomer equal to 18.6 kDa. Fig. 4B presents the p(r) obtained for LbHep1. The protein D_{max} and the frequency maximums were 130 Å and approximately 25 Å, demonstrating a quite elongated shape for LbHep1. Therefore, LbHep1 D_{max} is quite large for an 18.6 kDa protein. For instance, bovine serum albumin (BSA), which has a globular shape and is 66.4 kDa, has a D_{max} of approximately 110 Å [38]. As mentioned earlier in the text, CD data indicate that the LbHep1 N-terminal region seems to be unstructured while the C-terminal region is folded (Fig. 2). Thus, it is reasonable to infer that there are some flexible regions on the protein, and those regions appear to be in N-terminus of the protein. We hypothesize that this region is responsible for the LbHep1 elongated shape. Conversely, the C-terminal region, which contains the ZBM, might be folded and compact.

Together, these hydrodynamic and structural data demonstrated that LbHep1 is an elongated monomer in solution. Interestingly, hHep1 monomer presents a f/f_0 of approximately 1.4, which is also similar for the predicted value of yHep1 [18]. Therefore, LbHep1 has a higher elongated shape than hHep1, although we observed that LbHep1 also presents solubilization function over mtHsp70 of humans (data not shown). Therefore, the shape of LbHep1 differs from the shape reported for hHep1 and yHep1 [18,35].

Interestingly, the elongated shape that was observed for LbHep1 seems to be a characteristic of several Hsp70 co-chaperones. We have demonstrated this property for several Hsp70 co-chaperones such as Hsp40 [39,40], human mitochondrial GrpEs [41,42] and *L. braziliensis* Hsp70-interacting protein [43]. In all of these cases, the co-chaperone D_{max} is the same size or higher than what was reported for Hsp70 [17] and may allow a co-chaperone to interact with both Hsp70 domains.

3.6. The presence of zinc ion is critical for LbHep1 secondary and tertiary structures

To investigate the effect of the zinc ions in the LbHep1 structure, we removed these ions from LbHep1 samples by exhaustive dialysis against EDTA solution followed by a second dialysis to extract the excess EDTA. Fraga et al. [44], demonstrated that zinc ions are critical to maintain the secondary structure of truncated yHep1, and the same effect was observed for LbHep1. After the aforementioned treatment, the absence of zinc ions caused changes in the CD spectrum suggesting its importance for maintaining the secondary structure of LbHep1 (Fig. 5A).

Another strategy tested was monitoring the LbHep1 fluorescence emission spectra upon EDTA titration (Fig. 5B). The presence of 10 mM EDTA caused changes in the LbHep1 local tertiary structure, because the fluorescence emission spectrum suffered a red-shift change, suggesting that the LbHep1 tryptophan located near the ZBM became more solvated (Fig. 5B – *inset*). Upon EDTA titration, the <λ> values measured for LbHep1 increased until it reached a plateau near 10 mM EDTA and remained constant up to 100 mM EDTA (Fig. 5B). Moreover, the EDTA saturation was not sufficient to completely chemically unfold LbHep1 because a further red-shift change was reached in the presence of GndHCl (Fig. 5B – *inset*).

To evaluate the importance of Zn^{2+} ions for LbHep1 stability, we performed chemical-induced unfolding experiments followed by intrinsic fluorescence emission in the absence and the presence of 10 mM EDTA. This concentration was chosen because it was the

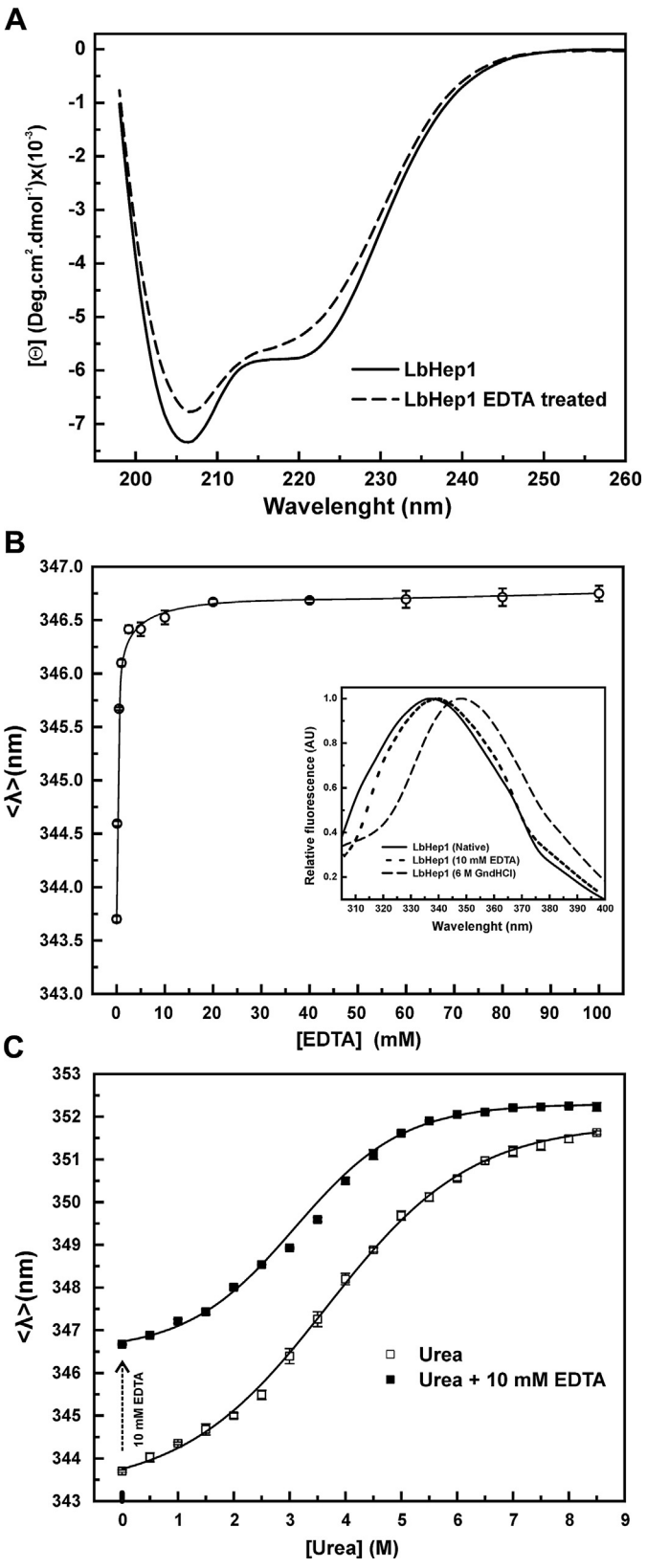

Fig. 5. LbHep1 needs zinc ions for structuration and stabilization. (A) CD spectra of LbHep1 with and without Zn^{2+} ions. Spectra changes in the absence of Zn^{2+} ions indicate that they contribute to LbHep1 secondary structure content. (B) LbHep1 <λ> value variation upon EDTA titration indicated that removing Zn^{2+} ions from the protein altered the local tertiary structure. *Inset*: effect of EDTA and urea on the LbHep1 fluorescence emission spectrum. (C) Variation of the <λ> value for LbHep1 upon titration of urea (0–8.5 M) in the absence and the presence of 10 mM EDTA. The Cms were 3.7 ± 0.1 M and 3.1 ± 0.1 M urea in the absence and the presence of EDTA, respectively.

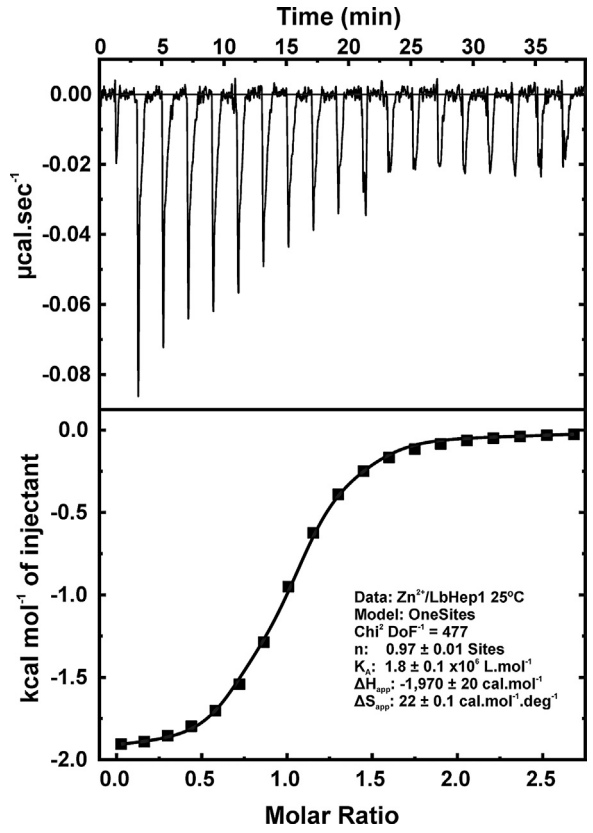

Fig. 6. Interaction of LbHep1 with Zinc ions evaluated by ITC. The experiment indicates that LbHep1 interacted with Zn^{+2} ion with a stoichiometry of 1:1 and revealed that both enthalpy and entropy direct the interaction. The K_A measured for this interaction pointed out a K_D of 0.6 μM, which was similar to that reported for the interaction of yHep1 with zinc ions. See text for details.

minimal EDTA concentration needed for the maximum change in the <λ values upon EDTA titration (Fig. 5B). Urea titration onto LbHep1 samples caused an apparent gradual transition of the measured <λ> values (Fig. 5C), suggesting the existence of more than one unfolding event. As observed above, the presence of 10 mM EDTA resulted in a 3 nm red-shift in the <λ> values, and the addition of the chemical denaturant led to additional red shift changes until we reached <λ> values similar to those that were measured for LbHep1 in the absence of EDTA. The chemical-induced unfolding experiments revealed that EDTA had a destabilizing effect on LbHep1, probably by chelating Zn^{2+} ions and their extraction from the protein as was also reported for hHep1 [18]. This effect can be observed by altering the midpoint concentration (Cm) of the LbHep1 chemical transition. In the case of urea, the Cm was reduced in the absence compared with the presence of 10 mM EDTA, from 3.7 M to 3.1 M. Therefore, Zn^{2+}-ion chelation caused changes in both the secondary and tertiary structures of LbHep1 in addition to reducing its chemical stability.

3.7. Interaction of LbHep1 with Zn^{2+} by isothermal titration calorimetry

The interaction of LbHep1 with Zn^{2+} ions was studied using ITC, which also allowed for determining some thermodynamic properties of the interaction. Fig. 6 demonstrates the thermogram concerning zinc sulfate titration in LbHep1 samples in its apo form, indicating that zinc binding to LbHep1 is exothermic. The thermodynamic signature (ΔH_{app} −1.970 ± 20 kCal mol^{-1} and ΔS_{app} 22 ± 0.1 kCal mol^{-1} K^{-1} at 25 °C) indicated that both enthalpy and entropy drive the interaction reaction. The ITC

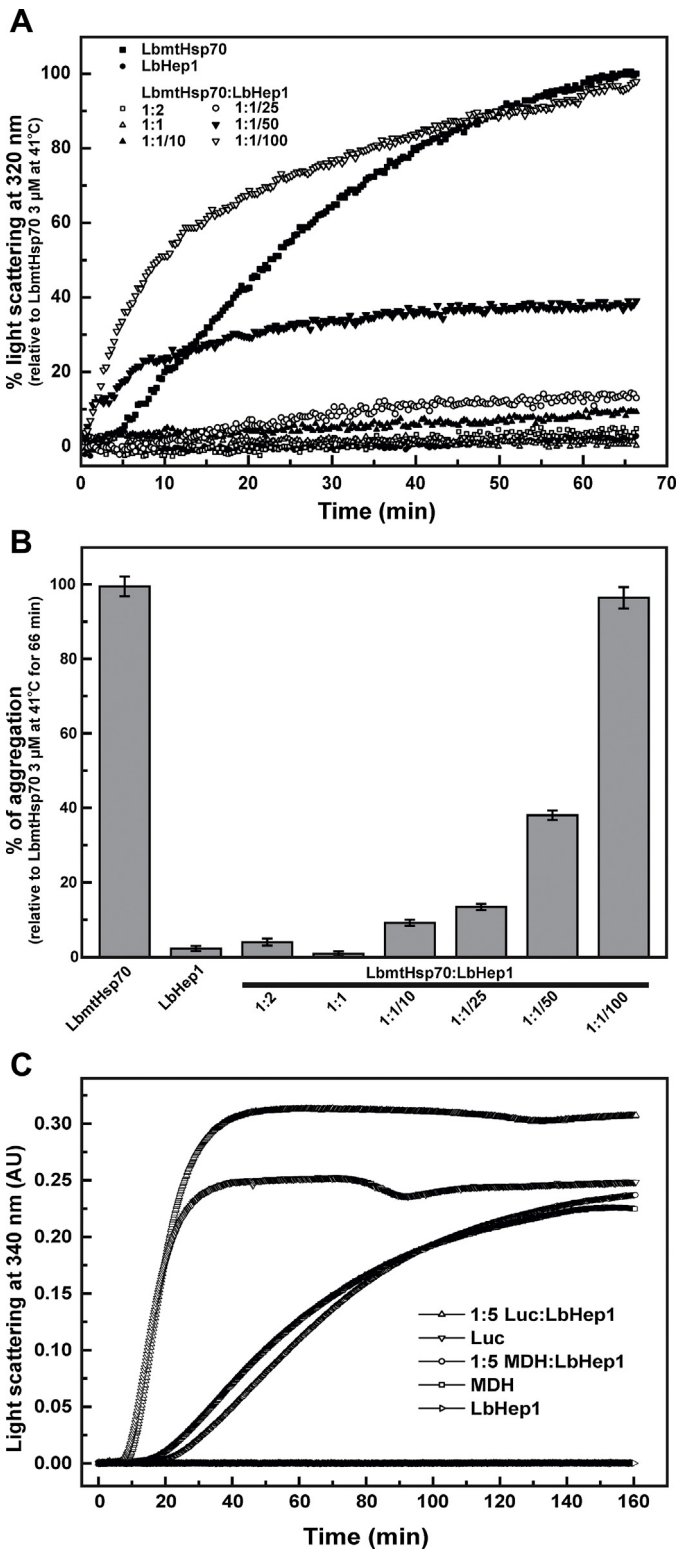

Fig. 7. LbHep1 prevented LbmtHsp70 thermal aggregation and LbHep1 chaperone activity. (A) LbmtHsp70 (3.0 μM) thermal aggregation was induced by incubation at 41 °C for 66 min and monitored by light scattering at 320 nm. Increasing concentrations of LbHep1 (0.03–6.0 μM) were added in LbmtHsp70 samples. At stoichiometric concentrations, LbHep1 avoided LbmtHsp70 aggregation indicating its protective effect. (B) Relative LbmtHsp70 aggregation after 66 min at 41 °C, indicating that LbHep1 prevented LbmtHsp70 thermal induced aggregation even in sub-stoichiometric concentrations. (C) LbHep1 has no significant chaperone activity on model client proteins. Thermal-induced protein aggregation of model client proteins was monitored at 340 nm, 40 °C for 160 min. The samples contained 1 μM MDH and Luc in the absence and the presence of LbHep1 (5 μM). See text for details.

experiment also revealed a 1:1 LbHep1:Zn^{2+} stoichiometry and a K_A of $1.8 \pm 0.1 \times 10^6$ L mol^{-1} and a K_D = 0.6 μM. Similar findings were reported by [44] with zinc titration to yHep1 containing EDTA. The reported thermodynamic parameters for yHep1, at 25 °C, were −1.9 kCal mol^{-1} and 23 kCal mol^{-1} K^{-1}, for ΔH_{app} and ΔS_{app}, respectively, while the K_A was 2.6×10^6 M^{-1} and K_D = 0.4 μM [44]. Although the experiments with LbHep1 and yHep1 have been conducted differently, zinc titration into protein samples comprised zinc binding to LbHep1 both in its apo form and EDTA free conditions as well as yHep1 containing an excess of EDTA. These results indicate that the "interaction strength" of zinc in protein has the same order of magnitude, and the thermodynamic parameters that direct the interaction are similar. Interestingly, Fraga et al., [44] indicates that Zn^{2+} is essential for yHep1 function in preventing SSC1 aggregation and that the metal coordination is coupled to the protein folding process. Therefore, yHep1 structure is intrinsically dependent on Zn^{2+} coordination. Based on the similarities between the thermodynamic properties for interaction between Zn^{2+} with LbHep1 or yHep1, both proteins interact with Zn^{2+} similarly suggesting a common interaction mechanism and a similar structural scaffold.

3.8. LbHep1 prevents LbmtHsp70 aggregation

The *in vitro* LbHep1 functionality was evaluated by protective action in preventing the LbmtHsp70 thermal induced aggregation. The effect of LbHep1 was assessed by increasing LbHep1 concentrations in LbmtHsp70 samples (constant concentration of 3.0 μM). The result presented in Fig. 7A shows that LbHep1 prevented the time-dependent LbmtHsp70 thermal aggregation at stoichiometric concentrations. In contrast, LbmtHsp70 without LbHep1 demonstrated time-dependent aggregation while LbHep1 presented a neglected aggregation propensity at high concentrations. Further, LbHep1 prevented LbmtHsp70 thermal induced aggregation even at sub-stoichiometric concentrations (Fig. 7A and B) indicating that LbHep1 interaction with LbmtHsp70 is transient. Only at 0.03 μM LbHep1 (100 times less LbHep1 concentration than LbmtHsp70), LbmtHsp70 reached similar maximum aggregation to that observed in the absence of the co-chaperone.

To assess whether the aggregation prevention by LbHep1 is specific to LbmtHsp70, we evaluated the intrinsic chaperone activity of LbHep1 in aggregation prevention assays of model client proteins such as MDH and Luc. As shown in Fig. 7C, LbHep1 did not present chaperone activity to MDH and Luc. There were not significant differences in the LbHep1 concentrations tested (data not shown); therefore, Fig. 7C only illustrates the molar ratio of 1:5. Apparently, LbHep1 co-aggregated with Luc because its presence increased light scattering while LbHep1 alone did not demonstrate thermal-induced aggregation. This phenomenon may be due to a nonspecific interaction of LbHep1 with hydrophobic residues of this client protein. In conclusion, LbHep1 has no intrinsic chaperone activity, but it presented a protective effect upon the LbmtHsp70 thermal-induced aggregation, indicating that it acts as a specific chaperone for LbmtHsp70.

4. Conclusion

LbHep1 is an essential co-chaperone for LbmtHsp70 viability as demonstrated in our co-expression experiments. LbHep1 truncation mutant co-expression with LbmtHsp70 demonstrated that the zinc finger domain is critical for LbmtHsp70 solubilization. The CD data indicated that the truncated mutant covering the N-terminal region of LbHep1 is unstructured while the C-terminal region is folded. These data suggest that the zinc finger domain is responsible for the LbHep1 secondary structure content. LbHep1

is a highly elongated monomer, probably due to the unstructured N-terminal region. But this is also a recurrent characteristic that is observed for other Hsp70 co-chaperones and may be important letting the co-chaperone to interact with both Hsp70 domains and allow for fine regulation of the Hsp70 molecular cycle.

The zinc ion, when removed from the recombinant LbHep1, cause changes in its chemical stability, probably because zinc depletion weakens the secondary and tertiary structure. Moreover, LbHep1 interacts with zinc ion with high affinity and presents a thermodynamic signature similar to the interaction of yHep1 with zinc ion, indicating that they share a similar scaffold for this interaction.

Functionally, we demonstrate *in vitro* that LbHep1 inhibits the self-aggregation of LbmtHsp70 in sub-stoichiometry fashion, even at a temperature above that of human physiology (37 °C) and the vector insect (25 °C). These findings are important because they indicate that LbHep1 is critical for LbmtHsp70 activity. LbHep1 also prevented the thermally induced aggregation of LbmtHsp70 but not that of the model client protein, such as MDH and Luc, suggesting that it is a specific chaperone for LbmtHsp70. Considering the key role of LbmtHsp70 in the installation and adaptation of parasites in the host, we can infer that any disturbance in LbHep1 protein can interrupt the LbmtHsp70 activity. Therefore, it is a potential target for new therapy design.

Acknowledgments

J.C. Borges thanks FAPESP (Fundação de Amparo à Pesquisa do Estado de São Paulo) and CNPq (Conselho Nacional de Desenvolvimento Científico e Tecnológico) for financial support (grants #2007/05001-4, #2011/23110-0, 2014/07206-6 and #471415/2013-8) and Research Fellowship grants (#306125/2012-9). L.R.S. Barbosa also thanks CNPq for financial support (#303048/2012-3). P.R. Dores-Silva thanks FAPESP for post-doc fellowship (#2014/16646-0). We acknowledge the Spectroscopy and Calorimetry Laboratory at Brazilian Biosciences National Laboratory (LNBio/CNPEM-ABTLuS, Campinas, Brazil) for making available the AUC device. We also thank the Brazilian Synchrotron Light Laboratory (LNLS/CNPEM-ABTLuS, Campinas, Brazil) for the use of the SAXS beamline. We thank MSc. Thiago V. Seraphim for critical reading of the manuscript.

Appendix A. Supplementary data

Supplementary data associated with this article can be found, in the online version, at http://dx.doi.org/10.1016/j.ijbiomac.2015.05.042

References

[1] J. Alvar, I.D. Velez, C. Bern, M. Herrero, P. Desjeux, J. Cano, J. Jannin, M.W. den Boer, L.C. Team, Leishmaniasis worldwide and global estimates of its incidence, PLoS ONE 7 (2012).
[2] T.V. Seraphim, C.H.I. Ramos, J.C. Borges, The interaction networks of Hsp70 and Hsp90 in the Plasmodium and Leishmania parasites, in: W.A. Houry (Ed.), The Molecular Chaperones Interaction Networks in Protein Folding and Degradation, Springer, New York, 2014, pp. 445–481.
[3] R. Pallavi, N. Roy, R.K. Nageshan, P. Talukdar, S.R. Pavithra, R. Reddy, S. Venketesh, R. Kumar, A.K. Gupta, R.K. Singh, S.C. Yadav, U. Tatu, Heat shock protein 90 as a drug target against protozoan infections. Biochemical characterization of hsp90 from *Plasmodium falciparum* and *Trypanosoma evansi* and evaluation of its inhibitor as a candidate drug, J. Biol. Chem. 285 (2010) 37964–37975.
[4] A. Shonhai, A.G. Maier, J.M. Przyborski, G.L. Blatch, Intracellular protozoan parasites of humans: the role of molecular chaperones in development and pathogenesis, Protein Pept. Lett. 18 (2011) 143–157.
[5] L.H. Van der Ploeg, S.H. Giannini, C.R. Cantor, Heat shock genes: regulatory role for differentiation in parasitic protozoa, Science 228 (1985) 1443–1446.
[6] R. Larreta, M. Soto, L. Quijada, C. Folgueira, D.R. Abanades, C. Alonso, J.M. Requena, The expression of HSP83 genes in *Leishmania infantum* is affected by temperature and by stage-differentiation and is regulated at the levels of mRNA stability and translation, BMC Mol. Biol. 5 (2004) 3.
[7] M. Bente, S. Harder, M. Wiesgigl, J. Heukeshoven, C. Gelhaus, E. Krause, J. Clos, I. Bruchhaus, Developmentally induced changes of the proteome in the protozoan parasite *Leishmania donovani*, Proteomics 3 (2003) 1811–1829.
[8] F.S.V. Matrangolo, D.B. Liarte, L.C. Andrade, M.F. de Melo, J.M. Andrade, R.F. Ferreira, A.S. Santiago, C.P. Pirovani, R.A. Silva-Pereira, S.M.F. Murta, Comparative proteomic analysis of antimony-resistant and susceptible *Leishmania braziliensis* and *Leishmania infantum* chagasi lines, Mol. Biochem. Parasitol. 190 (2013) 63–75.
[9] F.U. Hartl, A. Bracher, M. Hayer-Hartl, Molecular chaperones in protein folding and proteostasis, Nature 475 (2011) 324–332.
[10] K.P. da Silva, J.C. Borges, The molecular chaperone Hsp70 family members function by a bidirectional heterotrophic allosteric mechanism, Protein Pept. Lett. 18 (2011) 132–142.
[11] S. Priya, S.K. Sharma, P. Goloubinoff, Molecular chaperones as enzymes that catalytically unfold misfolded polypeptides, FEBS Lett. 587 (2013) 1981–1987.
[12] P. Dolezal, V. Likic, J. Tachezy, T. Lithgow, Evolution of the molecular machines for protein import into mitochondria, Science 313 (2006) 314–318.
[13] M. Bohnert, N. Pfanner, M. van der Laan, A dynamic machinery for import of mitochondrial precursor proteins, FEBS Lett. 581 (2007) 2802–2810.
[14] M. Horst, W. Oppliger, S. Rospert, H.J. Schonfeld, G. Schatz, A. Azem, Sequential action of two Hsp70 complexes during protein import into mitochondria, EMBO J. 16 (1997) 1842–1849.
[15] P.J. Kang, J. Ostermann, J. Shilling, W. Neupert, E.A. Craig, N. Pfanner, Requirement for Hsp70 in the mitochondrial matrix for translocation and folding of precursor proteins, Nature 348 (1990) 137–143.
[16] K. Mapa, M. Sikor, V. Kudryavtsev, K. Waegemann, S. Kalinin, C.A. Seidel, W. Neupert, D.C. Lamb, D. Mokranjac, The conformational dynamics of the mitochondrial Hsp70 chaperone, Mol. Cell 38 (2010) 89–100.
[17] P.R. Dores-Silva, L.R.S. Barbosa, C.H.I. Ramos, J.C. Borges, Human mitochondrial Hsp70 (mortalin): shedding light on ATPase activity, interaction with adenosine nucleotides, solution structure and domain organization, PLOS ONE 10 (2015) e0117170.
[18] P.R. Dores-Silva, K. Minari, C.H. Ramos, L.R. Barbosa, J.C. Borges, Structural and stability studies of the human mtHsp70-escort protein 1: an essential mortalin co-chaperone, Int. J. Biol. Macromol. 56 (2013) 140–148.
[19] M. Sichting, D. Mokranjac, A. Azem, W. Neupert, K. Hell, Maintenance of structure and function of mitochondrial Hsp70 chaperones requires the chaperone Hep1, EMBO J. 24 (2005) 1046–1056.
[20] M.T. Vu, P. Zhai, J. Lee, C. Guerra, S. Liu, M.C. Gustin, J.J. Silberg, The DNLZ/HEP zinc-binding subdomain is critical for regulation of the mitochondrial chaperone HSPA9, Protein Sci. 21 (2012) 258–267.
[21] H. Yamamoto, T. Momose, Y. Yatsukawa, C. Ohshima, D. Ishikawa, T. Sato, Y. Tamura, Y. Ohwa, T. Endo, Identification of a novel member of yeast mitochondrial Hsp70-associated motor and chaperone proteins that facilitates protein translocation across the inner membrane, FEBS Lett. 579 (2005) 507–511.
[22] L. Burri, K. Vascotto, S. Fredersdorf, R. Tiedt, M.N. Hall, T. Lithgow, Zim17, a novel zinc finger protein essential for protein import into mitochondria, J. Biol. Chem. 279 (2004) 50243–50249.
[23] C. Diaz de la Loza Mdel, M. Gallardo, M.L. Garcia-Rubio, A. Izquierdo, E. Herrero, A. Aguilera, R.E. Wellinger, Zim17/Tim15 links mitochondrial iron-sulfur cluster biosynthesis to nuclear genome stability, Nucleic Acids Res. 39 (2011) 6002–6015.
[24] F. Willmund, M. Hinnenberger, S. Nick, M. Schulz-Raffelt, T. Muhlhaus, M. Schroda, Assistance for a chaperone – Chlamydomonas HEP2 activates plastidic HSP70B for cochaperone binding, J. Biol. Chem. 283 (2008) 16363–16373.
[25] P. Zhai, C. Stanworth, S. Liu, J.J. Silberg, The human escort protein hep binds to the ATPase domain of mitochondrial Hsp70 and regulates ATP hydrolysis, J. Biol. Chem. 283 (2008) 26098–26106.
[26] J. Kluth, A. Schmidt, M. Marz, K. Krupinska, R. Lorbiecke, Arabidopsis zinc ribbon 3 is the ortholog of yeast mitochondrial HSP70 escort protein HEP1 and belongs to an ancient protein family in mitochondria and plastids, FEBS Lett. 586 (2012) 3071–3076.
[27] M.G. Claros, P. Vincens, Computational method to predict mitochondrially imported proteins and their targeting sequences, Eur. J. Biochem. 241 (1996) 779–786.
[28] J. Lebowitz, M.S. Lewis, P. Schuck, Modern analytical ultracentrifugation in protein science: a tutorial review, Protein Sci. 11 (2002) 2067–2079.
[29] P. Schuck, M.A. Perugini, N.R. Gonzales, G.J. Howlett, D. Schubert, Size-distribution analysis of proteins by analytical ultracentrifugation: Strategies and application to model systems, Biophys. J. 82 (2002) 1096–1111.
[30] J.C. Borges, C.H.I. Ramos, Analysis of molecular targets of *Mycobacterium tuberculosis*by analytical ultracentrifugation, Curr. Med. Chem. 18 (2011) 1276–1285.
[31] D. Orthaber, A. Bergmann, O. Glatter, SAXS experiments on absolute scale with Kratky systems using water as a secondary standard, J. Appl. Crystallogr. 33 (2000) 218–225.
[32] D.I. Svergun, Determination of the regularization parameter in indirect-transform methods using perceptual criteria, J. Appl. Crystallogr. 25 (1992) 495–503.

[33] F.A. Batista, G.S. Almeida, T.V. Seraphim, K.P. Silva, S.M. Murta, L.R. Barbosa, J.C. Borges, Identification of two p23 co-chaperone isoforms in *Leishmania braziliensis* exhibiting similar structures and Hsp90 interaction properties despite divergent stabilities, FEBS J. 282 (2015) 388–406.
[34] T.V. Seraphim, L.M. Gava, D.Z. Mokry, T.C. Cagliari, L.R.S. Barbosa, C.H.I. Ramos, J.C. Borges, The C-terminal region of the human p23 chaperone modulates its structure and function, Arch. Biochem. Biophys. 565 (2015) 57–67.
[35] T. Momose, C. Ohshima, M. Maeda, T. Endo, Structural basis of functional cooperation of Tim15/Zim17 with yeast mitochondrial Hsp70, EMBO Rep. 8 (2007) 664–670.
[36] I. Lewrenz, N. Rietzschel, B. Guiard, R. Lill, M. van der Laan, W. Voos, The functional interaction of mitochondrial Hsp70s with the escort protein Zim17 is critical for Fe/S biogenesis and substrate interaction at the inner membrane preprotein translocase, J. Biol. Chem. 288 (2013) 30931–30943.
[37] L.K. Sanjuan Szklarz, B. Guiard, M. Rissler, N. Wiedemann, V. Kozjak, M. van der Laan, C. Lohaus, K. Marcus, H.E. Meyer, A. Chacinska, N. Pfanner, C. Meisinger, Inactivation of the mitochondrial heat shock protein Zim17 leads to aggregation of matrix Hsp70s followed by pleiotropic effects on morphology and protein biogenesis, J. Mol. Biol. 351 (2005) 206–218.
[38] R. Itri, W. Caetano, L.R.S. Barbosa, M.S. Baptista, Effect of urea on bovine serum albumin in aqueous and reverse micelle environments investigated by small angle X-ray scattering, fluorescence and circular dichroism, Braz. J. Phys. 34 (2004) 58–63.
[39] J.C. Silva, J.C. Borges, D.M. Cyr, C.H.I. Ramos, I.L. Torriani, Central domain deletions affect the SAXS solution structure and function of yeast Hsp40 proteins Sis1 and Ydj1, BMC Struct. Biol. 11 (2011) 40.
[40] J. Borges, H. Fischer, A. Craievich, C. Ramos, Low resolution structural study of two human HSP40 chaperones in solution – DjA1 from subfamily A and DjB4 from subfamily B have different quaternary structures, J. Biol. Chem. 280 (2005) 13671–13681.
[41] C. Oliveira, J. Borges, I. Torriani, C. Ramos, Low resolution structure and stability studies of human GrpE#2, a mitochondrial nucleotide exchange factor, Arch. Biochem. Biophys. 449 (2006) 77–86.
[42] J. Borges, H. Fischer, L. Hansen, A. Craievich, C. Ramos, Free human mitochondrial GrpE is a symmetric dimer in solution, J. Biol. Chem. 278 (2003) 35337–35344.
[43] P.R. Dores-Silva, E.R. Silva, F.E.R. Gomes, K.P. Silva, L.R.S. Barbosa, J.C. Borges, Low resolution structural characterization of the Hsp70-interacting protein – Hip – from *Leishmania braziliensis* emphasizes its high asymmetry, Arch. Biochem. Biophys. 520 (2012) 88–98.
[44] H. Fraga, E. Papaleo, S. Vega, A. Velazquez-Campoy, S. Ventura, Zinc induced folding is essential for TIM15 activity as an mtHsp70 chaperone, Biochim. Biophys. Acta 1830 (2013) 2139–2149.